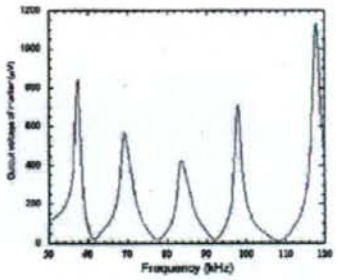

Fig. 7 Frequency of the induced voltage of five markers.

Table 1 Each marker.

	Marker 1	Marker 2	Marker 3	Marker 4	Marker 5
Inductance (mH)	5.6	5.4	5.6	5.1	5.7
Capacitance (nF)	1.3	0.97	0.64	0.52	0.32
Resonant frequency (kHz)	57.5	69.5	83.5	98.0	118.0

Table 2 Position accuracy.

	Marker 1	Marker 2	Marker 3	Marker 4	Marker 5
xy plane	0.5	0.4	0.8	0.2	0.5
yz plane	0.8	0.7	0.5	1.0	1.0
total	0.9	0.8	0.9	1.0	1.1

Unit: mm

接続した，3軸のマイクロメータにより正確に移動させた．近接したマーカ間の距離は約20mmとした．

Fig. 7はマーカの誘導電圧の周波数依存性を示したものである．誘導電圧がピークとなる周波数はそれぞれ57.5 kHz，69.5 kHz，83.5 kHz，98.0 kHz，118.0kHzであった．Table 1には5個のマーカのインダクタンス，キャパシタンス，共振周波数を示した．本計測システムにおける振幅および位相の計測確度は，測定周期が0.1秒(10Hz)であれば，振幅確度は約1.7 μ V，位相確度は5.1 mdegreeであり，SN比は最大で100程度であった．

Fig. 8はFig. 5(a)に示すように5個のマーカをアクリル棒に固定して同時に移動させた時の各マーカの中心位置を示したものである．それぞれのマーカは約20mmずつ離して配置した．マーカはFig. 5(a)のyz平面内で30mm × 30mmの正方形にマイクロメータを用いて移動させた．30mm × 30mmの移動距離は指の動きの範囲を目安として設定した．最も左に配置したマーカをmarker1とし，隣接する順にmarker2，marker3，marker4，marker5とした．Fig. 8(a)はmarker1の軌跡を表し，Fig. 8(b)，Fig. 8(c)，Fig. 8(d)，Fig. 8(e)はそれぞれmarker2，marker3，marker4，marker5の軌跡を表している．各軌跡はyz平面およびxy平面への射影をそれぞれ示した．計測周期は10Hzとした．●はシステムによって得られたマーカの中心位置であり，実線は理論値を示している．マイクロメータの移動方向とシステムのxyz軸は一致していないため，yz平面への軌跡の射影は若干平行四辺形になり，xy平面への射影は理想的な直線からはずれている．理論値は一辺30mmの正方形を実測された平行四辺形に近い軌跡と

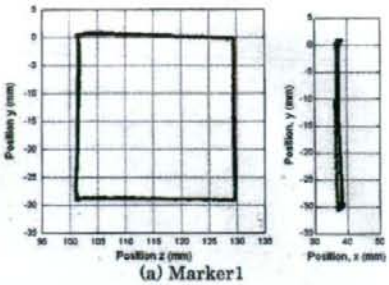

(a) Marker1

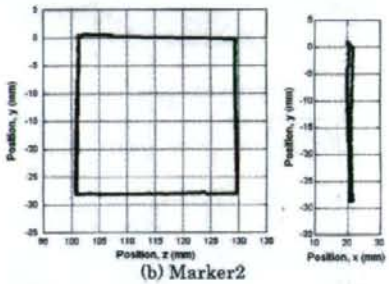

(b) Marker2

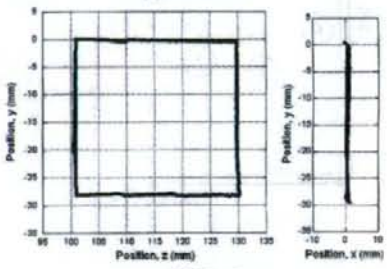

(c) Marker3

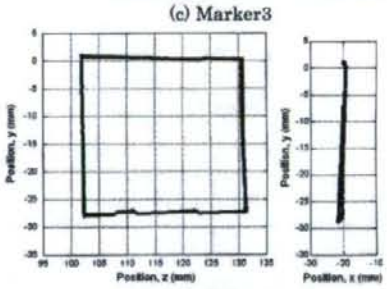

(d) Marker4

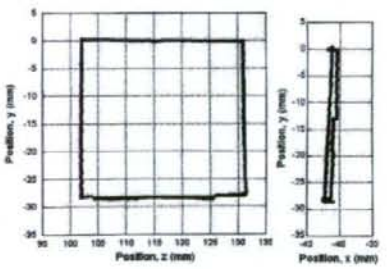

(e) Marker5

Fig. 8 Profile of five markers.

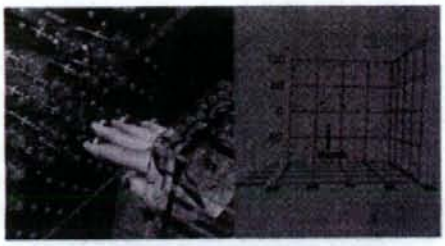

(a) Bending thumb

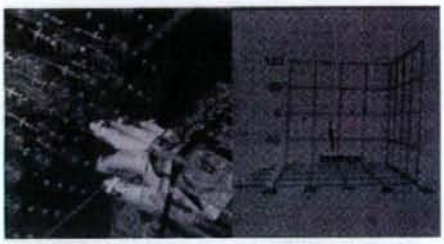

(b) Bending forefinger

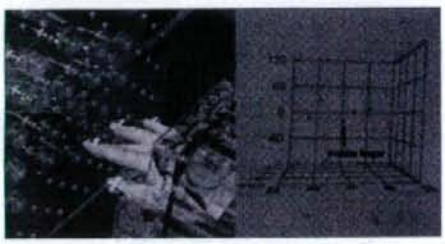

(c) Bending middle finger

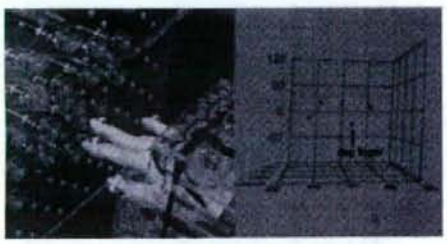

(d) Bending ring finger

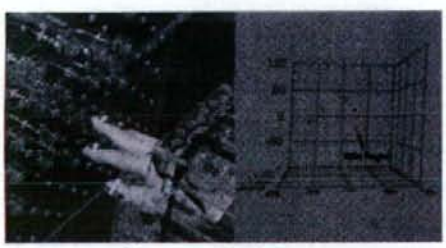

(e) Bending little finger

Fig. 9 Measured positions of fingertips.

なるように傾けた軌跡として求めた．yz 平面の軌跡では y 方向の変位量が 30mm よりも小さい値になっており，これは実際の磁気マーカの軌跡が x 軸方向へ若干傾いているためと考えられる．5 個のマーカにおいて，システムから得られた位置は理論的な軌跡とほぼ一致し，5 個のマーカの位置は同時かつ正確に計測できていることが了解される．

Table 2 はそれぞれマーカの位置精度を示したものである．位置精度は xy 平面および yz 平面において実測された軌跡と理論的な軌跡の最大の誤差を求め，全体の位置精度は xy 平面の精度と yz 平面の精度の相乗平均から算出した．Fig. 8 における一辺 30mm の正方形の移動距離において，相対位置精度は 1.1mm 以内であった．誤差要因としてはマーカが相互に接近しているために相互インダクタンスが共振周波数のずれとして計測され[8]，それが位置精度を悪化させているものと考えられる．

4.2 指先のモーションキャプチャ

Fig. 9 は各指先に貼付したマーカの写真および各マーカの位置を表示した動画の一部を静止画として表示したものである．各マーカの表示は Fig. 5 の z 軸の負方向から xy 平面を見る向きとした．5 個のマーカは手袋をはめた状態で各指の先端付近に貼り付けた．親指から順番に 1 本ずつ曲げる動作を繰り返した．(a) は親指のみを曲げた状態，(b) (c) (d) (e) はそれぞれ人差し指，中指，薬指，小指のみを曲げた状態をあらわしている．システムで得られた 5 個のマーカの位置はそれぞれの右側に点で表示されている．指先の位置は正確に計測されていることが了解される．計測速度は 20 Hz であり，指の通常の動きはほぼリアルタイムで計測可能であった．

5. まとめ

1. 5 個の共振型磁気マーカの位置検出システムを開発した．
2. 指先の運動範囲を想定した 30mm × 30mm の正方形の各辺において 5 個同時にマーカを移動させた場合の位置精度は 1.1mm 以内であった．
3. 指先にマーカを貼付して，リアルタイムに指先の位置を計測できるモーションキャプチャシステムを開発した．最高 20Hz で指先の動きを計測できた．

謝辞

PXI 計測システムの作製にご協力いただいた株式会社 CPI テクノロジーズ　高野卓雄氏，高野卓大氏，鎌田　勇氏に感謝いたします．本研究の一部は総務省の「戦略的情報通信研究開発推進制度」（5E5 番 126 号）の助成により行った．

References

1) http://www.solidray.co.jp/product/hanryoku/index.html.

2)http://www.nihonbinary.co.jp/Virtual/5DT/index.htm.
3)H. Sasaki, T. Kuroda, Y. Manabe, and K. Chihara, *Journal of the Virtual Reality Society of Japan*, vol. **7**, pp. 393-402 (2002).
4)J.A. Paradiso, K. Hsiao, J. Stricken, J. Lifton, A. Adler, *IBM Systems Journal*, vol. **39**, No. 3&4, pp. 892-914 (2000).
5) S. Yabukami, S. Hashi, Y. Tokunaga, T. Kohno, K.I. Arai, and Y. Okazaki, *Journal of the Magnetics Society of Japan*, vol. **28**, pp. 877-885 (2004).
6) S. Yabukami, T. Katoh, S. Hashi, K.I. Arai, and Y. Okazaki, *Journal of the Magnetics Society of Japan*, vol. **30**, pp. 218-224 (2006).
7) J.E. Mcfee, Y. Das, *IEEE Trans. Antennas and Propagation*, vol. **AP-29**, pp. 282-287(1981).
8) Nakagawa, Y. Koyanagi, Experimental Data Analysis by the least square method ,p.95-99, The University of Tokyo Press (1982).
9)S. Hashi, Y. Toyoda, S. Yabukami, K. Ishiyama, Y. Okazaki, and K. I. Arai, *IEEE Transactions on Magnetics*, vol. 43, pp. 2364-2366 (2007).

2007年5月10日受理，2007年9月11日採録

Available online at www.sciencedirect.com
ScienceDirect
Sensors and Actuators A 142 (2008) 520–527
SENSORS AND ACTUATORS A PHYSICAL
www.elsevier.com/locate/sna

Wireless magnetic motion capture system using multiple LC resonant magnetic markers with high accuracy

Shuichiro Hashi [a,*], Masaharu Toyoda [a], Shin Yabukami [b], Kazushi Ishiyama [c], Yasuo Okazaki [a], Ken Ichi Arai [d], Hiroyasu Kanetaka [e]

[a] Department of Materials Science and Technology, Gifu University, 1-1 Yanagido, Gifu 501-1193, Japan
[b] Department of Electrical Engineering and Information Technology, Tohoku Gakuin University, 1-13-1 Chuo, Tagajo 985-8537, Japan
[c] Research Institute of Electrical Communication, Tohoku University, 2-1-1 Katahira, Aoba-ku, Sendai 980-8577, Japan
[d] The Research Institute for Electric and Magnetic Materials, 2-1-1 Yagiyama-minami, Taihaku-ku, Sendai 982-0807, Japan
[e] Graduate School of Dentistry, Tohoku University, 4-1 Seiryo-machi, Aoba-ku, Sendai 980-8575, Japan

Received 22 January 2007; received in revised form 17 August 2007; accepted 12 September 2007
Available online 26 September 2007

Abstract

The present paper reports the principle of a wireless magnetic motion capture system that uses multiple LC resonant magnetic markers and demonstrates its application. Small and lightweight markers (4 mm in diameter, 10 mm in length, and 0.63 g in weight) use a soft ferrite core and a coil, representing a minimal LC circuit with no battery, driven wirelessly by electromagnetic induction. The markers are given respective resonant frequencies ranging from 150 to 450 kHz. The magnetic signal of the marker is detected by a pick-up coil array consisting of 25 pick-up coils. The markers are excited by a superposed wave corresponding to all of the resonant frequencies, while the voltage signals induced through pick-up coils are separated in a frequency spectrum by FFT analysis. Regardless of the number of markers, the voltage amplitude for each resonant frequency can be easily obtained simultaneously, and thus the proposed system can detect multiple markers. In addition, the positional error of the system caused by a mutual inductance between the exciting coil and the LC marker was examined. The impedance change of the exciting coil due to a resonance of the LC marker was found to perturb the strength of the magnetic field used for marker excitation. The closer a marker approaches the exciting coil, the larger it becomes. This fluctuation induces an error in the marker signal, which is measured by the pick-up coils and is necessary for positional calculation. Then, considering the mutual inductance, a compensatory process was employed for positional calculation in order to improve the positional accuracy. After compensation, the absolute positional accuracy was determined to be less than 2 mm within 140 mm of the pick-up coil array.

Keywords: Wireless magnetic motion capture system; LC resonant magnetic marker; Multi-position detection; Positional orientional accuracy

1. Introduction

Close range motion capture is thought to be a useful technique for developing a next-generation virtual input device. For these applications, a small and lightweight wireless, wearable marker is strongly desired so that motions of the arms or fingers are not disturbed. The system must also be able to individually detect invisible objects in optically shielded space. However, in such cases, conventional and widely used optical methods cannot detect the marker. Magnetic motion capture systems are believed to satisfy these requirements. Several investigations to determine the position and orientation of a magnetic object or source have been reported [1–7]. However, conventional systems require that the magnetic object be large compared to the marker or that the marker contain electric wiring, in order to obtain a high SN ratio for the magnetic signal from the marker. Therefore, we previously proposed a wireless magnetic motion capture system using a magnetically coupled LC resonant magnetic marker [8–10]. In addition, we developed a wireless multi-marker detecting system using LC resonant magnetic markers [11]. The proposed system was shown to detect up to five markers simultaneously and to allow the approximate orientations and positions of the markers to be determined accurately to within 2 mm in a space located 100 mm from the pick-up coil array. However, a unique

* Corresponding author. Tel.: +81 58 293 2722; fax: +81 58 293 2722.
E-mail address: hashi@gifu-u-.ac.jp (S. Hashi).

0924-4247/$ – see front matter © 2007 Elsevier B.V. All rights reserved.
doi:10.1016/j.sna.2007.09.011

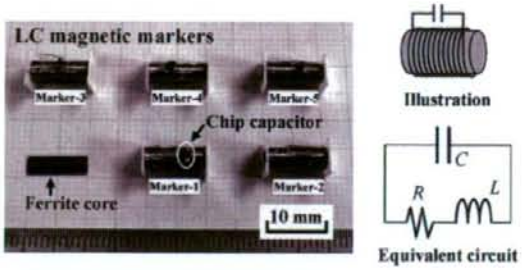

Fig. 1. Photograph and schematic diagram of the LC resonant magnetic marker.

detection error occurs with increased distance from the pick-up coil array.

In the present paper, we evaluate the positional and orientational accuracy of the proposed system with respect to the attitude angle of the markers. We herein examine the detection error and extend the detectable space with high accuracy for detecting the positions and orientations of the markers.

2. System component and signal acquisition

Fig. 1 shows a photograph and a schematic diagram of the LC resonant magnetic markers. The marker consists of a Ni–Zn ferrite core (3 mm in diameter and 10 mm in length) with a wound coil and a chip capacitor, representing an LC series circuit. Five markers, designed for resonant frequencies of 157, 202, 273, 323, and 440 kHz, respectively, were prepared. Table 1 shows the specifications of each LC marker, and the quality factor of each LC marker is approximately 70. A schematic diagram of the newly developed motion capture system is shown in Fig. 2. The system is composed of measurement equipment and a coil assembly consisting of an exciting coil and an array of newly designed pick-up coils. The pick-up coil array consists of 25 pick-up coils placed at intervals of 45 mm on an acryl board. Each coil consists of 40 turns of polyester enameled copper wire (PEW) wound around an acryl bobbin of 25 mm in diameter. An excitation voltage of 44 V_{p-p} is applied to the driving coil (10 turns of PEW around a 390 mm × 390 mm Teflon coil) and the markers are strongly excited at its resonant frequency by electromagnetic induction. However, the system becomes slow as the number of markers increases, owing to the time required to switch frequencies and make multiple measurements. Therefore, a superposed wave including all of the resonant frequency components of the markers is used to realize simultaneous excitation. As shown in Fig. 3, the induced voltage wave measured by the pick-up coils is analyzed in each frequency spectrum by

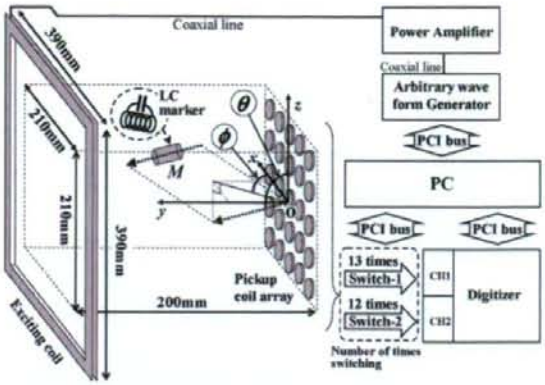

Fig. 2. Schematic diagram of the proposed wireless motion capture system for performance verification.

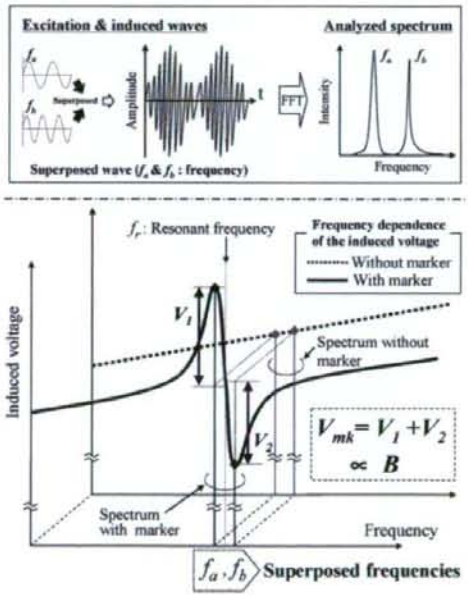

Fig. 3. Signal of LC marker acquisition technique (superposed wave excitation and FFT analysis).

FFT analysis. The spectra are first measured without the marker and are then measured with the marker. The induced voltage of the marker contributes V_{mk}, which can be obtained by vector subtraction of the amplitude of the spectrum without the marker

Table 1
Specifications of the LC resonant magnetic markers

	Marker-1	Marker-2	Marker-3	Marker-4	Marker-5
Resonant frequency [kHz]	157	202	273	323	440
Coil turns	350	300	270	220	120
Inductance [μH]	1184	914	734	510	140
Chip capacitor [pF]	910	680	470	470	910
Quality factor	70	70	70	65	72

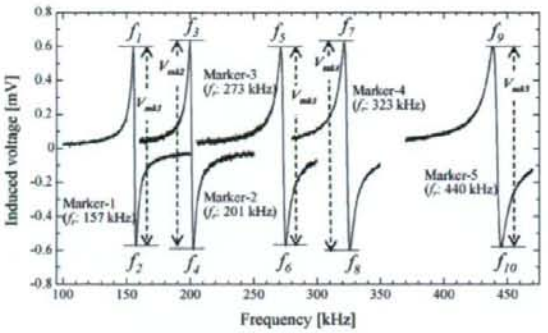

Fig. 4. Induced voltages due to the excitation of five markers.

from the amplitude of spectrum with the marker. The amplitude V_{mk} measured by each pick-up coil varies in proportion to the flux density B that the marker produces for the location of the pick-up coil. Fig. 4 shows the frequency dependence of the induced voltage from the markers. Sharp signals due to LC resonance of the markers were observed, and there was no influence on neighboring signals from the skirts of each signal. In practice, the superposed wave, which is composed of 10 frequencies corresponding to the upper and lower peaks (f_1–f_{10}), shown in Fig. 4 is used for excitation.

3. Calculation of position and orientation

The position and orientation of the markers is obtained by solving an inverse problem; more than six values (in this paper, 25 values are used) of the flux density at known locations are needed to determine both the position and orientation of the marker as the magnetic flux source (six degrees of freedom). To solve this problem, the flux density generated from the marker is considered as a magnetic dipole field. Based on this assumption, the position and orientation of the marker is calculated using the following equations (Eqs. (1)–(3)) and the nonlinear method of least squares, which effect an optimization using the Gauss–Newton method [12].

$$S(\vec{p}) = \sum_{i=1}^{n} \left\| \vec{B}_{\text{meas}}^{(i)} - \vec{B}_{\text{cal}}^{(i)}(\vec{p}) \right\|^2 \rightarrow \text{Minimum} \tag{1}$$

$$\vec{B}_{\text{cal}}^{(i)}(\vec{p}) = \frac{1}{4\pi\mu_0} \left\{ -\frac{\vec{M}}{r_i^3} + \frac{3(\vec{M}\vec{r}_i)\vec{r}_i}{r_i^5} \right\} \tag{2}$$

$$\vec{p} = (x, y, z, \theta, \phi, M) \tag{3}$$

Here, $S(\vec{p})$ is the objective function (the residual sum of squares), i is the coil number, n is the total number of coils, $\vec{B}_{\text{meas}}^{(i)}$ is the measured flux density, $\vec{B}_{\text{cal}}^{(i)}$ is the theoretical flux density that takes the magnetic dipole field into account, $\vec{p}$ is the parameters of the marker, $\vec{M}$ is the magnetic moment, and $\vec{r} = (x, y, z)$ is the position of the marker. Eq. (2) is the equation of an ideal dipole field expressed as a function of position and orientation. In the present paper, as shown in Fig. 2, position and orientation of the marker is expressed in polar coordinates: ϕ is the angle between the x-axis and the direction vector when the moment is projected onto the xy-plane, and θ is the angle between the direction of the moment and the z-axis.

4. Evaluation results of the system

4.1. Distance and attitude dependency of the markers

The position accuracy was verified experimentally for the system. As shown in Fig. 5, the positional and orientational accuracies were evaluated at attitude angles of $\phi = 90°$ (parallel to the y-axis) and $\phi = 135°$ when the five markers were lined up in five ranks at 20-mm intervals. The markers were swept from $y = 60$ to 140 mm in 10-mm steps along the y-axis in the xy-plane at $z = -50$, 0, and 50 mm, respectively. Fig. 6 shows the detected positions displayed in three dimensions. When all of the markers were parallel to the y-axis ($\phi = 90°$), approximately correct positions were obtained. A maximum positional deviation of approximately 5 mm was observed for markers located at (80, 140, 50), (80, 140, 0), and (80, 140, −50), whereas, as shown in Fig. 7, the intervals between adjacent markers were less than 3 mm in terms of relative positional accuracy. The relative error of the measured position of all of the points at intervals between adjacent markers was evaluated and expressed as an

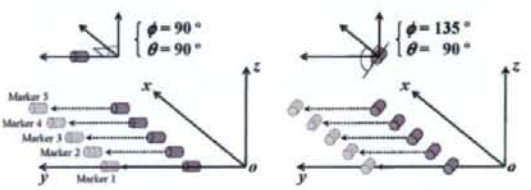

Fig. 5. Arrangement of the LC markers for evaluation of the system.

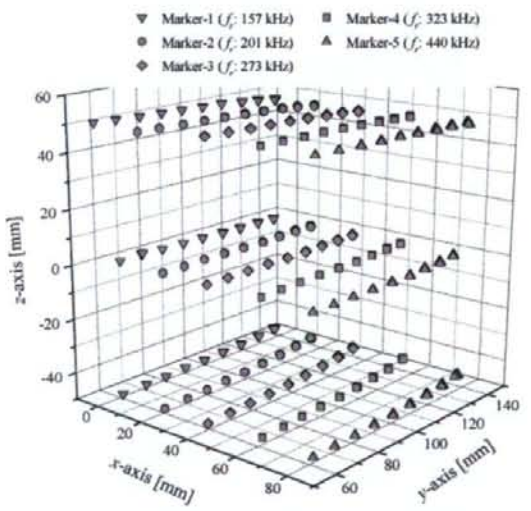

Fig. 6. Evaluation results of detected position (displayed in three dimensions).

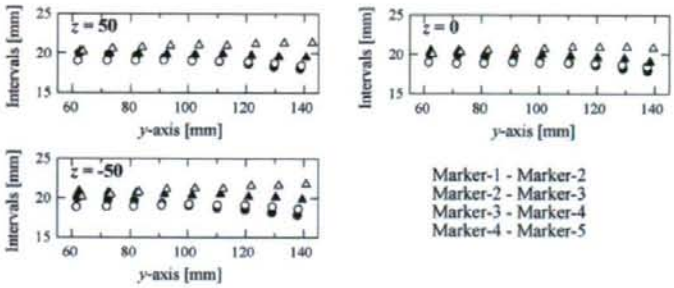

Fig. 7. Intervals between adjacent markers.

averaged value with a standard deviation. The results are as follows: 19.03 ± 0.88 mm at Mk1-2 (interval between Marker 1 and Marker 2), 18.79 ± 0.25 mm at Mk2–3, 19.88 ± 0.65 mm at Mk3–4, and 20.55 ± 0.41 mm at Mk4–5. The increase in the detection error for large distances is thought to be due to the relationship between the size and the arrangement of the exciting coil and the pick-up coil array.

Fig. 8(a) and (b) shows the detected positions and orientations, respectively, at $z=0$ displayed in two dimensions at $\phi=90°$ (parallel to the y-axis) and $\phi=135°$, where each point represents 100 measurements at each marker position. The detected results for $\phi=90°$ are represented by filled circles and those for $\phi=135°$ are represented by open triangles. As shown in Fig. 8, at $\phi=90°$, the solutions converged to a certain state of less than 1 mm in 100 measurements, and the position accuracies for each marker were within 2 mm. Approximately correct orientations were acquired at $\phi=90°$ when the markers were located up to 100 mm from the pick-up coil array. In contrast, at $\phi=135°$, the repeatable position and orientation accuracies become worse up to 5 mm and 5 degrees, respectively. Furthermore, the position and the orientation in detected values scatter in all directions for approximately 10–15 mm as the marker position is positioned more than 100 mm from the pick-up coil array. This is due to the fact that the marker is not excited efficiently at these positions, degrading the SN ratio, because the deviation angle between the exciting field vector and the normal vector of

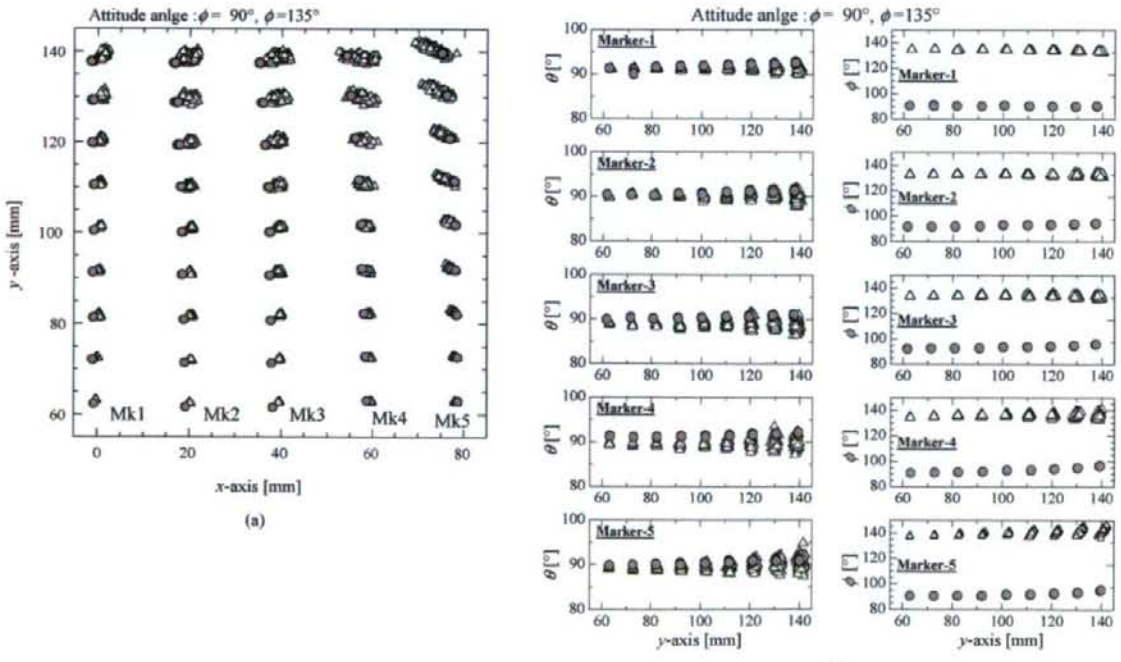

Fig. 8. Positional and attitude angle accuracies for different attitude of the marker. (a) Positional accuracy on the xy-plane and (b) accuracies of attitude angles θ and ϕ.

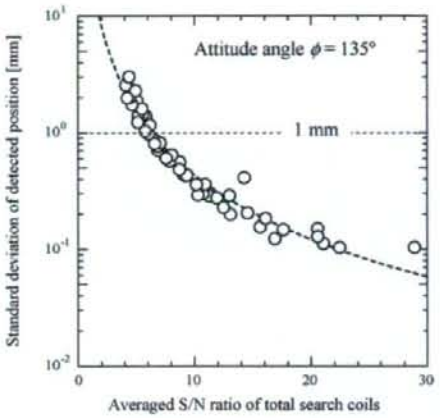

Fig. 9. Positional unevenness as a function of the S/N ratio.

the marker approach a right angle. In the xy-planes in which z is not equal to zero, since the actual positions of the marker with $\phi = 135°$ were departing from the center of pick-up coils array, the scattering tendency of the detected positions, as in Fig. 8, were observed.

Fig. 9 shows the relationship between the averaged SN ratio of the pick-up coil array and the repeatable position accuracy at an attitude angle of $\phi = 135°$ to indicate the amount of scatter in measured values. The noise level of the system was estimated to be 1 μV. The repeatable accuracy degraded as the averaged SN ratio decreased.

Overall, the results show that the system is capable of capturing the motion of the markers wirelessly and with an accuracy on the millimeter scale when the cylinder axes of the markers are parallel with the exciting field. However, the accuracy in detection will become worse as the deviation between the attitude angles and the exciting field increases.

Since the system using ac magnetic field, a nonmagnetic and a nonmetallic environment are required to realize high detection accuracy. However, because the system is free from the influence of the earth magnetic field the large-scale shield system is not needed. In such an environment, the effect of a living body as a dielectric to the system under the frequency less than hundreds of kHz is also considered to be very small. To give an example, it is considered that the system can be applied to the orthodontics and the dentofacial orthopedics, if a planer type marker will be realized. In such applications, the measurement range is enough to capture the swing of the jaw.

4.2. Compensatory tracking of unique detection error

In order to clarify the increase in the detection error of the markers for large distances from the pick-up coil array, the evaluation has been performed experimentally as follows. The position and orientation were detected for a single marker parallel to the y-axis. As shown in Fig. 10, the marker was swept from $x = -90$ to 90 mm and from $y = 60$ to 140 mm in 10-mm steps along the grid pattern in the xy-plane at $z = 0$ and 90 mm

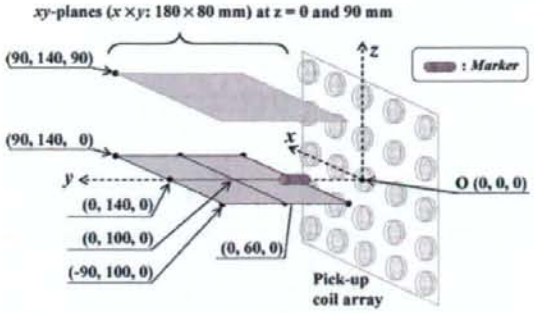

Fig. 10. Schematic diagram of the evaluation area.

(see Fig. 2 for the coordinate system). The movement of the marker was performed by a precision three-dimensional axial auto scanner with a positioning accuracy of less than 0.1 mm. The evaluation results are shown in Figs. 11 and 12. Each point represents 10 measurements at each marker position, where squares indicate actual positions, crosses indicate detected positions, and triangles indicate compensated positions, which will be described later. Good repeatable accuracy of within 1 mm is seen in Figs. 11(a) and 12(a). However, the detected positions were gradually deflected towards the y-axis along the broken lines in Fig. 11(a) (the center axis of the pick-up coil array) as the marker moved away from the pick-up coil array and approached the exciting coil. The deflection of the detected positions was also observed in the yz-plane at $z = 90$ mm, as shown in Fig. 12(c). In addition, Figs. 11(d) and 12(e) show that the deviation of the attitude angle ϕ in the xy-plane rotates anti-clockwise from 90° along the positive x-axis and rotates clockwise from 90° along the negative x-axis gradually up to approximately 10°. In the case of $z = 90$ mm, similar rotations of the attitude angle ϕ are also observed for the angle θ, as shown in Fig. 12(d) (see Fig. 13 for the illustration).

Maximum positional deviation distances of approximately 7 mm were observed for the markers located at (−90, 140, 0) and (90, 140, 0). As mentioned earlier, the increase in the detection error for large distances is thought to be due to the relationship between the size and arrangement of the driving coil and the marker. Therefore, in order to address this problem, the mutual inductance between the exciting coil and the marker at a resonant point was calculated at every position of the marker and tried to compensate for the position and the orientation of the marker. In practice, the impedance change of the exciting coil due to the mutual inductance is considered to perturb the excitation field. As a result, as shown in Figs. 11 and 12, the compensated positions and orientations of the markers, indicated by triangles, agree well with the actual positions and orientations of the marker indicated by squares.

In practical use, the compensatory tracking of the positional error in real time is required for the system. It is necessary to know the actual position of the marker with respect to the exciting coil in order to estimate the electromagnetic coupling between the before detection. This is clearly inconsistent. Also, because the electromagnetic coupling depends on the distance

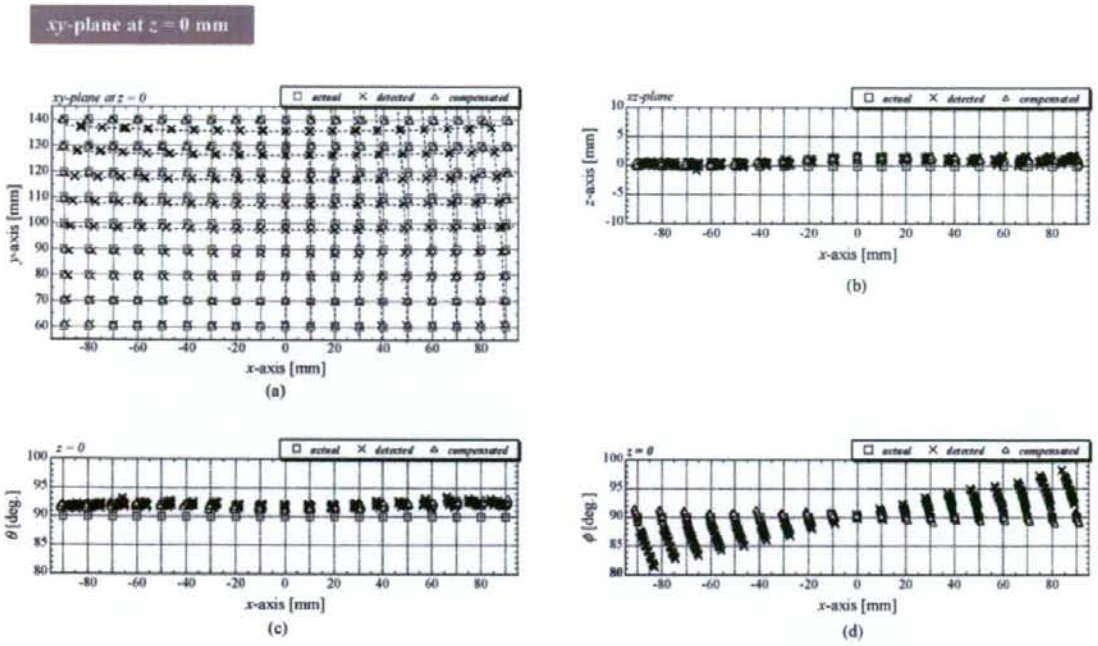

Fig. 11. Verification results of the positional accuracy at $z = 0$ mm displayed in (a) the xy-plane, (b) the xz-plane, and the attitude angles (c) θ and (d) ϕ.

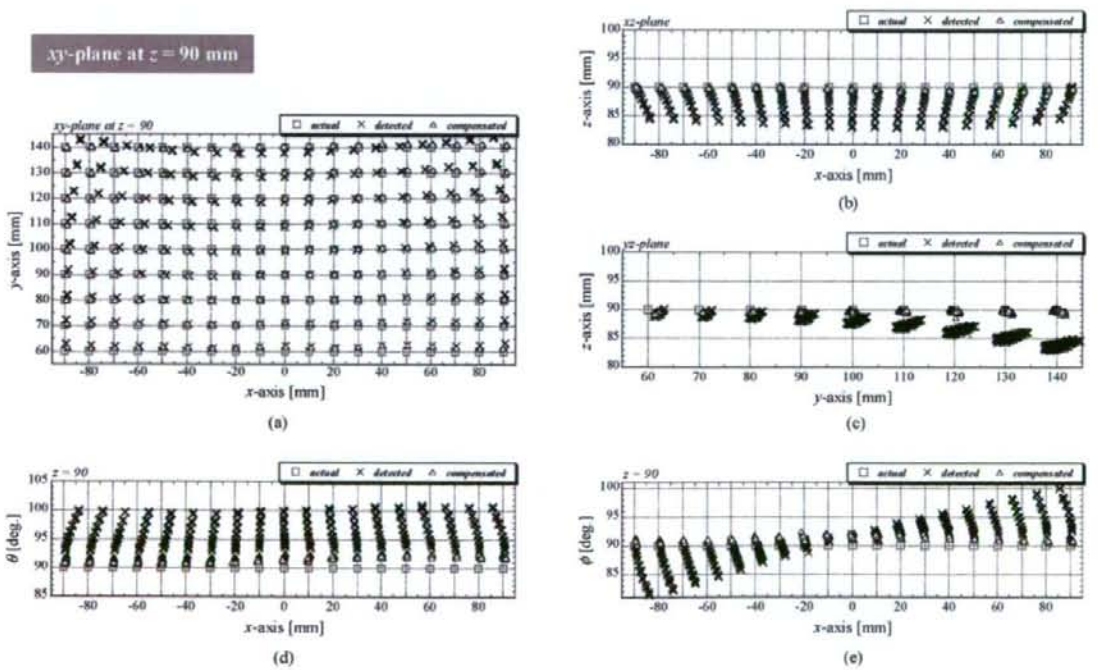

Fig. 12. Verification results of the positional accuracy at $z = 90$ mm displayed in (a) the xy-plane, (b) the xz-plane, and (c) the yz-plane, and the attitude angles (d) θ and (e) ϕ.

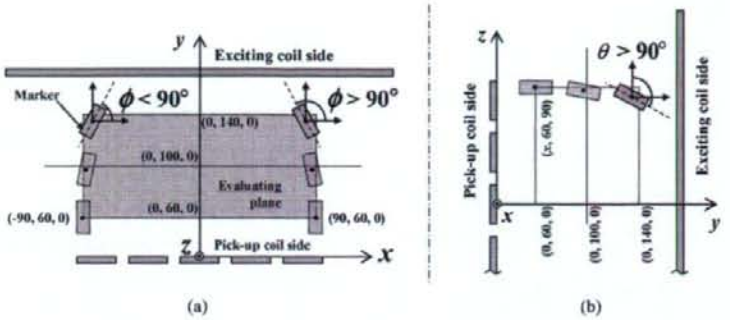

Fig. 13. Schematic diagram of the state of the detection error due to the influence of the mutual inductance. (a) A view of the *xy*-plane. (b) A view of the *yz*-plane.

and orientation of the LC markers to the exciting coil as mentioned before, the several excitation coils having different orientations are considered to be difficult to improve the influences of the electromagnetic coupling, although it will be useful for exciting the marker efficiently and improve the SN ratio of the system. However, the data of the coordinates comparatively close to the actual position, such as the initial values used in Eq. (1), can be employed. In addition, the equivalent circuit can shorten the calculation time. In practice, we adopted the compensatory tracking process for the system and evaluated the system. The results indicate that the accuracies of the compensation were approximately the same as the results shown in Figs. 11 and 12, and the supplementary time for the calculation was up to several milliseconds.

5. Conclusions

The performance of the proposed wireless magnetic motion capture system for five markers was evaluated. The LC resonant magnetic markers were given the individual resonant frequencies. The adoption of a superposed wave excitation and FFT analysis realized the simultaneous detection of multiple markers for the system. According to the attitude angle of the markers, the positional and orientational accuracies of the markers degrade as the distances of the markers from the pick-up coil array increase due to the decrease in the S/N ratio. The detectable accuracy of the markers was found to be less than 2 mm, and the approximate orientation of a marker could be determined when the markers were located within an area of 100 mm^3, up to 100 mm from the pick-up coil array. However, the deflection of the detected positions from the actual positions increased gradually as the distances of the markers from the pick-up coil array increased.

From the consideration of the mutual inductance between the exciting coil and the markers, the exact cause of the deflection was clarified, and the problem of the detectable space with high accuracy was solved. The impedance change of the exciting coil owing to the mutual inductance was found to perturb the excitation field. Although constant-current excitation is favorable for the system, this is an ideal case and, in practice, the compensatory tracking process is considered to be more effective. Using the proposed system, the positions of the markers can be distinguished to within less than 1 mm, and the absolute position accuracy for the marker is within 2 mm. Approximately correct orientations were obtained when the markers were located up to 140 mm from the pick-up coil array. These results indicate that the proposed system is capable of capturing the motion of markers wirelessly with high accuracy.

Acknowledgements

This study was supported in part by the Japan Society for the Promotion of Science (JSPS) through Grants-in-Aid for Scientific Research (B) Nos. 19300201 and 18360193, and by the Ministry of Health, Labour, and Welfare through a Grant-in-Aid for Scientific Research Project No. H18-Choujyu-Ippan-004.

References

[1] F. Grant, G. West, Interpretation Theory in Applied Geophysics, McGraw-Hill, New York, 1965, pp. 306–381.
[2] S.V. Marshall, IEEE Trans. Veh. Technol. VT-27 (1978) 65.
[3] W.M. Wynn, C.P. Frahm, P.J. Carroll, R.H. Clark, J. Wellhoner, M.J. Wynn, IEEE Trans. Magn. MAG-11 (1975) 701.
[4] F.H. Raab, E.B. Blood, T.O. Steiner, H.R. Jones, IEEE Trans. Aerosp. Electron. Syst. AES-15 (1979) 709.
[5] J.E. Mcfee, Y. Das, IEEE Trans. Antenn. Propag. AP-29 (1981) 282.
[6] J.A. Paradiso, K. Hsiao, J. Stricken, J. Lifton, A. Adler, IBM Syst. J. 39 (2000) 892.
[7] S. Yabukami, H. Kikuchi, M. Yamaguchi, K.I. Arai, K. Takahashi, A. Itagaki, N. Wako, IEEE Trans. Magn. 36 (2000) 3646.
[8] S. Yabukami, S. Hashi, Y. Tokunaga, T. Kohno, K.I. Arai, Y. Okazaki, J. Magn. Soc. Jpn. 28 (2004) 877.
[9] Y. Tokunaga, S. Hashi, S. Yabukami, T. Kohno, M. Toyoda, T. Ozawa, Y. Okazaki, K.I. Arai, J. Magn. Soc. Jpn. 29 (2005) 153.
[10] S. Hashi, Y. Tokunaga, S. Yabukami, M. Toyoda, K. Ishiyama, Y. Okazaki, K.I. Arai, IEEE Trans. Magn. 41 (2005) 4191.
[11] S. Hashi, M. Toyoda, S. Yabukami, K. Ishiyama, Y. Okazaki, K.I. Arai, IEEE Trans. Magn. 42 (2006) 3279.
[12] T. Nakagawa, Y. Koyanagi, Experimental Data Analysis by the Least Square Method, The University of Tokyo Press, Tokyo, 1982, pp. 95–99.

Biographies

Shuichiro Hashi received the DE degree in Electrical Engineering from Tohoku University, Japan, in 1998. He is an assistant professor in the Department of Materials Science and Technology, Gifu University. His research interests are in the area of applied magnetics, and magnetic materials.

Masaharu Toyoda received the ME degree in Electrical and Electronic Engineering from Gifu University, Japan, in 2007. He works now in Sony EMCS Corp.

Shin Yabukami received the DE degree in Electrical Engineering from Tohoku University, Japan, in 1998. He is an associate professor in the Department of Electrical Engineering and Information Technology, Tohoku Gakuin University. His research interests are in the area of magnetic sensor, and applied magnetics.

Kasuzhi Ishiyama received the PhD degree in Electrical Engineering from Tohoku University, Japan, in 1993. He is a professor in the Research Institute of Electrical Communication, Tohoku University. His research interests are in the area of magnetic actuators, and magnetic materials.

Yasuo Okazaki received the PhD degree from Tohoku University, Japan, in 1993. He is a professor in the Department of Materials Science and Technology, Gifu University. His research interests are in the area of magnetic shielding, and magnetic materials.

Ken Ichi Arai received the PhD degree in Electrical Engineering from Tohoku University, Japan, in 1971. He is a professor emeritus in Research Institute of Electrical Communication, Tohoku University and an administrator in the Research Institute for Electric and Magnetic Materials. His research interests are in the area of physical properties and application of magnetic materials.

Hiroyasu Kanetaka received the PhD degree in Dentistry from Tohoku University, Japan, in 1997. He is an associate professor in the Center for Research Strategy and Support (CRESS) and Graduate School of Dentistry, Tohoku University. His research interests are in the area of swallowing act.

Tohoku J. Exp. Med., 2008, **214**, 39-50

Beneficial Effects of Orthodontic Treatment on Quality of Life in Patients with Malocclusion

Shiori Azuma,[1] Masahiro Kohzuki,[2] Shuichi Saeki,[1] Mayumi Tajima,[3] Kaoru Igarashi[1] and Junji Sugawara[3]

[1]Department of Oral Dysfunction Science, Tohoku University Graduate School of Dentistry, Sendai, Japan
[2]Department of Internal Medicine and Rehabilitation Science, Tohoku University Graduate School of Medicine, Sendai, Japan
[3]Department of Orthodontics and Dentofacial Orthopedics, Tohoku University Graduate School of Dentistry, Sendai, Japan

Patients with malocclusion, especially those in need of surgical correction, have lower health related quality of life (HRQOL) and higher anxiety. We investigated the changes of HRQOL and psychological status following jaw surgery in the patients with facial deformities. Thirty-one adult orthodontic patients admitted to Tohoku University Hospital and diagnosed as malocclusion requiring jaw surgery were recruited for the study. The severity of malocclusion was assessed by Severity Score (SS) which is based on their cephalometric radiographs. They were divided into three groups according to the severity of malocclusion, i.e. Low-SS, Moderate-SS and High-SS. The subjects also completed a generic HRQOL (entire body health) instrument, and three disease-specific oral HRQOL instruments. HRQOL and psychological status of the patients were assessed before (T1) and at debonding of multibracketed appliances after surgery (T2). SS in each group significantly decreased to normal occlusion level (SS = 0~1). Oral function significantly improved from 11.8 ± 5.4 to 5.9 ± 4.3 in the Low-SS ($p < 0.01$), from 13.7 ± 6.5 to 8.8 ± 5.1 in the Moderate-SS ($p < 0.05$), and from 14.7 ± 6.7 to 7.8 ± 5.7 in the High-SS ($p < 0.01$). The patients after the surgical correction had improved disease-specific HRQOL and state anxiety irrespective of the severity before surgery, although the generic HRQOL, trait anxiety and depression were equal to that before the surgery. Furthermore, both postoperative anxiety and HRQOL were estimated by the preoperative anxiety and HRQOL. These results indicated that jaw surgery markedly improved the disease-specific HRQOL and psychological status in the present patients. We therefore suggest that assessments of the HRQOL and psychological status before treatment might predict the HRQOL and psychological status after the treatment to a certain extent. ——— psychological status; malocclusion; surgical correction; SF-36; severity score.

Tohoku J. Exp. Med., 2008, **214** (1), 39-50.

Received May 17, 2007; revision accepted for publication November 27, 2007.
Correspondence: Masahiro Kohzuki, M.D., Ph.D., Department of Internal Medicine and Rehabilitation Science, Tohoku University Graduate School of Medicine, 1-1 Seiryo-machi, Aoba-ku, Sendai 980-8574, Japan.
e-mail: kohzuki@mail.tains.tohoku.ac.jp

Oral diseases and disorders are highly prevalent and give rise to not only physical, but also economic, social, and psychological problems. They impair health related quality of life (HRQOL) and affect various aspects of life including function, appearance, and interpersonal relationships in a large number of individuals (Gift and Redford 1992).

In the past, oral HRQOL research was primarily directed at the assessment of the experiences of elderly patients who often suffer periodontal disease, tooth loss or inadequate dentures (Locker and Jokovic 1996; Inglehart and Bagramian 2002). Recently, oral HRQOL in children and adolescents has received considerable interest (Broder et al. 2002; Jokovic et al. 2002). Moreover, HRQOL assessments made by patients provide a view of dentofacial disharmony and surgical outcome that can inform clinicians in important ways (Bennett and Phillips 1999).

The patients' satisfaction with the orthodontic intervention is likely to be high when their initial dentofacial deformity is severe and have lower HRQOL and psychological status. We have recently reported that the patients with malocclusions especially in need of surgical correction had lower disease-specific HRQOL (Tajima et al. 2007). However, even after orthodontic treatment by the expert dentists, patients show large variations in the level of satisfaction (Kiyak et al. 1982; Flanary et al. 1990; Enomoto et al. 2000; Cunningham et al. 2002). Although preoperative HRQOL and phychological status of the patients might affect the level of satisfaction, prospective cohort study with the viewpoint has not been reported. Moreover, the predictors of HRQOL and psychological status after the treatment have not been elucidated. Therefore, in this study, we demonstrated the effects of orthodontic treatment on HRQOL and psychological status in the patients with facial deformities and also elucidated the predictors of better postoperative HRQOL and psychological status in the patients with facial deformities.

Material and Methods

Subjects

Eighty-one consecutive patients who had deformities in the maxilla and the mandible and had combined surgical-orthodontic treatment at the Tohoku University Hospital between April 2003 and December 2005 were included in the study. All of them filled in a questionnaire preoperatively and were asked to participate in the present study. The patients with any other co-morbidity or those who did not finish the treatment were excluded from the study. Exclusion criteria were the following : (1) any surgery performed in the previous days, (2) previous temporomandibular joint arthrotomies, (3) fewer than 20 teeth total or fewer than 10 teeth in each arch, (4) unstable residence or travel restrictions, (5) periodontal disease judged to be severe by the surgeon, (6) pregnancy, (7) previous mandibular surgery, and (8) inability to follow instructions or the study protocol. Finally, thirty-one patients who consented and finished the treatment were all analyzed in the study. All of them had single jaw or bimaxillary operations. Their ages ranged from 17.3 ~ 42.5 years with a mean age of 25.4. Approval for the study was given by the regional research ethics committee.

Persons with normal occlusion had good maxillomandibular relation, especially good bilateral canine relations and molar relations, and had adequate dental axis, overjet and overbite, and had no arch length discrepancy (ALD) or minor ALD (< 2 mm). To assess the patients' morphological deformities, we set up a Severity Score (SS) for each patient based on their cephalometric radiographs which were traced and lined, and the angular and plaster model measurements were assessed. The Severity Scores were used to assess the patients' dentofacial deformities, and defined in Table 1 (Tajima et al. 2007).

The characteristics of the subjects are shown in Table 2. The patients were divided into three groups according to the severity of malocclusion, i.e., Low-SS (SS 2 ~ 4; n = 13), Moderate-SS (SS 5; n = 11), and High-SS (SS 6 ~ 9; n = 7). There was no significant difference in gender and age among these three groups. Ability to speak and oral function of Low-SS were comparatively high in comparison with other groups and High-SS showed a tendency to be low. Generic HRQOL was assessed using The Short Form-36. Disease-specific HRQOL was evaluated with The Subjective Oral Health Status Indicators (SOHSI), The Orthognathic Quality of Life Questionnaire (OQLQ), and The Recognition and

TABLE 1. Definition of the severity score.

Dental	Arch length discrepancy (ALD)	0 : Deficiency≦ 7-8 mm 1 : Deficiency > 7-8 mm (7-8 mm: patient' own premolar size)
Skeletal	Anteroposterior jaw discrepancy (AD)	0 : Discrepancy ≦ 1 S.D. 1 : 1 S.D. < Discrepancy ≦ 2 S.D. 2 : 2 S.D. < Discrepancy ≦ 3 S.D. 3 : Discrepancy > 3 S.D.
Skeletal	Vertical jaw discrepancy (VD)	0 : Discrepancy ≦ 1 S.D. 1 : 1 S.D. < Discrepancy ≦ 2 S.D. 2 : 2 S.D. < Discrepancy ≦ 3 S.D. 3 : Discrepancy > 3 S.D.
Skeletal	Transversal jaw discrepancy (TD)	0 : Symmetry 1 : Asymmetry≦ 5 mm 2 : Asymmetry > 5 mm
	SS = Σ (ALD + AD + VD + TD)	(Minimum: 0, Maximum: 9) Normal occlusion: SS = 0~1

TABLE 2. Sample characteristics.

	Low-SS	Moderate-SS	High-SS
	(SS 2 ~ 4)	(SS 5)	(SS 6 ~ 9)
N (M, F)	13 (1, 12)	11 (3, 8)	7 (2, 7)
Mean age	26.1	26	24.3
(range)	(18.2 – 42.5)	(17.3 - 38.1)	(19.1 - 35.0)
Preoperative mean SS	3.4	5	6.4
Postoperative mean SS	0	0	0.4

SS, Severity Score; M, Male; F, Female.

Satisfaction scale modified (RSS-M) of surgical correction. In addition, anxiety and depression were assessed using STAI (Spielberger's State-Trait Anxiety Inventory Questionnaire) and SRQ-D (The Self-Rating Questionnaire for Depression), respectively. It took about 15-20 minutes for the patients to answer the questionnaire and no assistants helped them to answer the questionnaire. These generic and disease-specific HRQOL, anxiety and depression in patients were assessed just before surgery (T1) and after surgery involving debonding of multibracketed appliances (T2). The results compared the changes between pre and post intervention, and across three severity groups.

In addition, the patients were also analyzed in two groups, split according to degree of anxiety (High-anxiety, $n = 16$; Low-anxiety, $n = 15$) and depression (High-depression, $n = 14$; Low-depression, $n = 17$) scores before the intervention. The Anxiety and depression level between T1 and T2 were compared between the two groups.

The MOS Short Form-36 (SF-36)

The MOS Short Form-36 (SF-36) is a generic health status measure, and has been widely used (Ware and Sherbourne 1992; Garratt et al. 1996). The instrument consists of 36 items divided into eight subscales, namely:

physical functioning (PH), social functioning (SF), role physical (RP), role emotional (RE), vitality (VT), mental health (MH), bodily pain (BP) and general health (GH). Each scale is scored 0-100 where 0 is the worst possible and 100 the best possible health. There is good evidence for the validity, reliability, and responsiveness of SF-36 in different populations (Jenkinson et al. 1993; Garratt et al. 1994, 1996; Brazier et al. 1993).

Spielberger's State-Trait Anxiety Inventory Questionnaire (STAI)

The anxiety status was measured by Spielberger's State-Trait Anxiety Inventory Questionnaire (STAI) (Spielberger et al. 1970). Items for anxiety were selected for their ability to discriminate between stress and non-stress conditions. The state anxiety score (STAI-I) consists of 20 statements on a 4-point scale covering apprehension, tension, nervousness, and worry, which evaluates how the subjects feeling 'at this moment'. The trait anxiety score (STAI-II) consists of 20 statements on a 4-point scale pertaining to how the subjects generally feel. Both scales are designed to contain anxiety present and anxiety absent factors. The 20 responses for each scale are summed (Shumaker et al. 1990) and the total score for both ranges from 20 to 80, with a lower score reflecting a better psychological state.

The Self-Rating Questionnaire for Depression (SRQ-D)

The depression status was measured by the Self-Rating Questionnaire for Depression (SRQ-D) (Tsutsui 1993), which evaluates mild and more severe depressive conditions. The subjects tested have a choice of 4 answers to each question: seldom or never, some of time, quite often or almost always. For any one questions, these answers are scored 0, 1, 2 and 3, respectively. In scoring a completed questionnaire, the control items (6 items) are crossed out (Rockliff 1969) and the score ranges from 0 to 36, with a score of 11-16 representing borderline depression and a score above 16 representing depression (Tsutsui 1993). The reliability and validity of the questionnaires have been established and they have been used in a variety of clinical populations including patients with cardiac disease (Shumaker et al. 1990; Tsutsui 1993).

The Subjective Oral Health Status Indicators (SOHSI)

Disease specific HRQOL was measured by the Subjective Oral Health Indicators (SOHSI). The SOHSI takes as its theoretical basis Locker's conceptual model of oral health (Locker 1988). SOHSI is useful for descriptive oral health surveys of general populations. The instrument comprises the following scales: "Ability to chew (AC)" "Ability to speak (AS)" "Oral and facial pain symptoms (OFPS)" "Other oral symptoms (OOS)" "Eating impact scale (EIS)" "Communication/social relations impact scale (CSIS)" "Activities of daily living impact scale (ADIS)" and "Worry/concern impact scale (WCIS)". The response format varies with each scale. The scales "AC", "AS", "OFPC" and "OOS" all have a yes/no response format for their items. The "EIS", "ADIS" and the "WCIS" all have 5-point rating scales for the frequency of occurrence of each item with categories: all the time (scored 5), very often (scored 4), fairly often (scored 3), sometimes (scored 2) and never (scored 1). The measure has been shown to be reliable and valid in samples, both in Canada and UK (Locker 1997). All questions were administered as a self-complete questionnaire.

The Orthognathic Quality of Life Questionnaire (OQLQ)

Disease specific HRQOL was also measured by Orthognathic Quality of Life Questionnaire (OQLQ) (Cunningham et al. 2000). The instrument was developed for the orthognathic patients and consists of 22 statements marked on a 4-point scale according to how much the issue covered by the statement bothers the respondent. The 22 items contribute to four dimensions: "social aspects of dentofacial deformity (SA)" "facial aesthetics (FA)" "oral function (OF)" "awareness of dentofacial aesthetics (ADFA)". OQLQ dimensions are scored so that lower scores indicate a better quality of life and higher scores signify a poorer quality of life. The 100 mm visual analogue scale (VAS) is marked from 0 to 10; the respondents were asked to rate how they felt about their dental and facial appearance and oral function, with 0 being "no problem at all" and 10 being "the worst problem imaginable". The OQLQ showed good reliability (Cunningham et al. 2000), validity and responsiveness (Cunningham et al. 2002).

The Recognition and Satisfaction scale modified (RSS-M)

Patients' self-evaluation of their own facial parts was measured by the Recognition and Satisfaction Scale (RSS) (Enomoto et al. 2000). RSS consists of five domains. I used the following two domains: "recognition of facial deformity" and "self-evaluation of facial components". These two scales have 5-point rating scales of the degree of deformity or satisfaction of each item with

categories: much (scored 5), considerable (scored 4), mildly (scored 3), few (scored 2) and very little (scored 1). This measure showed good evidence of validity and responsiveness (Enomoto et al. 2000).

Data analysis

The results were expressed as the mean ± S.E.M. For statistical analysis, HRQOL data were analyzed by Wilcoxon signed rank test between T1 and T2. Comparisons among the 3 groups according to SS were performed using two-way factorial ANOVA. Comparisons between the groups were performed using Wilcoxon signed rank test. Logistic regression analysis was performed with the psychological status and the disease-specific HRQOL after surgery. A backward elimination procedure was used with a significance level of $\alpha = 0.05$ for staying in the model. The following variables obtained at T1 were entered as possible explanatory variables: "STAI-I", "STAI-II", "SRQ-D", "SA", "DFA", "OF", "ADFA", "Recognition", "Satisfaction", "Gender" and "Age". Females showed lower self-esteem and reduced satisfaction with body image (Kiyak et al. 1981). "Gender" was binary variables, and was therefore allocated values of 1 or 0 for male or female. Satisfaction with facial body image decreased with age (Cunningham et al. 2000). "Age" was treated as a continuous variable. Macintosh statistical package software, StatView 4.5 (Abacus Concepts, Inc., Berkeley, CA, USA) was used. $P < 0.05$ was considered statistically significant.

The study protocol was approved by the ethical committee of Tohoku University and all the subjects gave informed consent.

Results

Comparisons of HRQOL and psychological status among Low-SS, Moderate-SS, and High-SS

All patients' SS were improved almost completely (SS 0-SS 1) after the surgery (Table 2). Generic HRQOL measured by SF-36 is shown in Tables 3 and 4. There was no significant difference in any subscale scores of SF-36 between T1 and T2. Moreover, there was no significant difference in any subscale scores of SF-36 among Low-SS, Moderate-SS, and High-SS. Furthermore, there are data of the Japanese standard value under 29 years old of SF-36. There were no significant differences between the value of the subjects (T1 and T2) and the Japanese standard value (Table 3).

The psychological status measured by "STAI" and "SRQ-D" is shown in Table 3 and Table 4. In "STAI-I", there were significant differences between T1 and T2, ($p < 0.01$), however no significant differences were found in "STAI-II". There was no interaction among the SS groups. Moreover, no significant difference in "SRQ-D" was found. There was no interaction among the SS groups. When logistic regression was applied (Table 5), the predictor of postoperative "STAI-I" was preoperative "STAI-I" and "STAI-II" (53.6%, $p < 0.001$). The predictor of postoperative "SRQ-D" was preoperative "SRQ-D" and "STAI-I" (31.6%, $p < 0.01$). In contrast, it was difficult to predict the postoperative "STAI-I" by the preoperative anxiety and disease-specific HRQOL.

The disease-specific HRQOL measured by "SOHSI" is shown in Table 3 and Table 4. There were significant differences between T1 and T2, in "AC", "AS", "EIS (%) (sum)", "CSIS (%) (sum)", "ADIS (%) (sum)" and "WCIS (%) (sum)" of "SOHSI" ($p < 0.01$ or 0.05). However, there was no interaction among the three groups.

The disease-specific HRQOL measured by OQLQ is also shown in Tables 3, 4 and Fig. 1. There were significant differences between T1 and T2 in 3 out of 4 domains of OQLQ: "SA", "FA" and "OF". In contrast, there were no significant differences in "ADFA". There was interaction among the three groups. When logistic regression was applied (Table 5), the predictor of postoperative "SA" was the preoperative "SA" (28.5%, $p < 0.01$). The predictor of postoperative "FA" was the preoperative "OF", "SA", "STAI-I" and "STAI-II" (32.1%, $p < 0.01$). The predictor of postoperative "OF" was the preoperative "STAI-I", "STAI-II" and "gender" (35.0%, $p < 0.01$). The predictor of postoperative "ADFA" was the preoperative "STAI-I" (34.5%, $p < 0.01$).

The result of RSS-M is shown in Tables 3 and 4. Both in the domains of "Recognition" and "Satisfaction" there were significant differences between T1 and T2 ($p < 0.001$). There was no interaction among the groups. When logistic

TABLE 3. Comparisons of QOL and psychological status between T1 and T2.

Measure	Domain	T1	T2	Japanese standard (≦ 29y)
SF-36	Physical functioning (PF)	95.3 ± 8.50	96.4 ± 6.20	94.4 ± 9.40
	Role physical (RP)	89.5 ± 26.4	95.9 ± 18.3	91.9 ± 20.8
	Bodily pain (BP)	83.0 ± 21.4	86.0 ± 15.5	79.8 ± 21.2
	Social functioning (SF)	87.3 ± 15.5	84.9 ± 15.3	86.5 ± 18.9
	General health (GH)	57.9 ± 15.2	64.0 ± 16.5	71.3 ± 18.2
	Vitality (VT)	86.9 ± 15.6	84.4 ± 15.3	64.9 ± 19.6
	Role emotional (RE)	86.9 ± 25.4	84.8 ± 25.7	84.3 ± 27.5
	Mental health (MH)	68.1 ± 14.6	70.5 ± 15.1	70.5 ± 18.3
STAI & SRQ-D	State anxiety (STAI-I)	47.4 ± 8.80	39.4 ± 6.2**	
	Trait anxiety (STAI-II)	46.8 ± 8.50	45.0 ± 9.9	
	Depression (SRQ-D)	10.1 ± 3.80	9.5 ± 4.8	
SOHSI	Ability to chew (AC)	13.4 ± 16.8	5.9 ± 11.0*	
	Ability to speak (AS)	51.6 ± 42.0	22.5 ± 33.7*	
	Oral and facial pain symptoms (OFPS)	16.1 ± 18.3	18.4 ± 14.8	
	Other oral symptoms (OOS)	17.7 ± 11.7	15.8 ± 12.0	
	Eating impact scale (EIS) %	67.7 ± 37.0	38.7 ± 35.5**	
	Eating impact scale (EIS) sum	11.4 ± 2.75	13.2 ± 2.18**	
	Communication/social relations impact scale (CSIS) %	49.1 ± 30.6	22.5 ± 25.2**	
	Communication/social relations impact scale (CSIS) sum	16.4 ± 2.79	18.8 ± 1.63**	
	Activities daily living impact scale (ADIS) %	28.4 ± 32.5	12.3 ± 25.0*	
	Activities daily living impact scale (ADIS) sum	27.6 ± 3.00	29.1 ± 1.66*	
	Worry/concern impact scale (WCIS) %	90.3 ± 20.0	59.6 ± 35.1**	
	Worry/concern impact scale (WCIS) sum	5.87 ± 2.24	8.32 ± 1.70**	
OQLQ	Social aspects of dentofacial deformity (SA)	11.5 ± 8.8	4.5 ± 5.0**	
	Facial aesthetics (FA)	9.9 ± 5.1	3.0 ± 3.2**	
	Oral-function (OF)	13.1 ± 6.0	7.3 ± 4.9**	
	Awareness of dentofacial aesthetics (ADFA)	7.1 ± 4.4	5.2 ± 4.3	
RSS-M	Recognition	23.9 ± 5.7	13.2 ± 6.6**	
	Satisfaction	17.3 ± 5.3	30.5 ± 6.5**	

Generic quality of life was measured by SF-36 (The MOS Short Form-36). Psychological status was measured by STAI (State-Trait Anxiety Inventory Questionnaire) and SRQ-D (Self-Rating Questionnaire for Depression). Disease specific quality of life was measured by SOHSI (The Subjective Oral Health Indicators), OQLQ (The Orthognathic Quality of Life Questionnaire), and RSS-M (The Recognition and Satisfaction scale Modified). T1: before surgery, T2: after debonding of multibracket appliance. Results expressed as mean ± standard error (S.E.M.). *Significantly different from T1 by Wilcoxon signed rank test; $p < 0.05$. **Significantly different from T1 by Wilcoxon signed rank test; $p < 0.01$.

TABLE 4. Comparisons of QOL and psychological status among Low-SS, Moderate-SS and High-SS.

Measure	Domain	Low-SS (n = 13)		Moderate-SS (n = 11)		High-SS (n = 7)		Interaction
		T1	T2	T1	T2	T1	T2	P
SF-36	Physical functioning (PF)	95.0 ± 8.10	96.5 ± 4.2	96.3 ± 8.90	96.3 ± 8.9	94.2 ± 9.7	95.0 ± 7.6	0.98
	Role physical (RP)	90.3 ± 16.2	92.3 ± 27.7	90.9 ± 30.1	97.7 ± 7.5	85.7 ± 37.7	100 ± 0	0.72
	Bodily pain (BP)	87.3 ± 15.9	85.8 ± 15.3	81.7 ± 23.0	89.0 ± 14.4	77.0 ± 28.3	81.7 ± 18.7	0.71
	Social functioning (SF)	87.3 ± 13.5	85.3 ± 14.4	88.5 ± 19.8	81.6 ± 14.2	85.4 ± 13.4	89.2 ± 19.6	0.61
	General health (GH)	58.7 ± 16.4	68.8 ± 15.4	56.7 ± 12.1	58.8 ± 16.9	58.4 ± 20.2	63.2 ± 18.1	0.69
	Vitality (VT)	87.3 ± 13.5	85.3 ± 14.4	88.5 ± 19.8	81.6 ± 14.2	83.0 ± 12.9	87.5 ± 20.9	0.60
	Role emotional (RE)	86.9 ± 21.2	81.9 ± 29.4	84.7 ± 31.2	81.6 ± 27.5	85.5 ± 26.4	95.1 ± 12.8	0.61
	Mental health (MH)	70.4 ± 11.3	70.4 ± 14.0	67.6 ± 17.4	72.7 ± 15.0	64.5 ± 16.7	67.4 ± 18.8	0.84
STAI & SRQ-D	State anxiety (STAI-I)	48.0 ± 10.2	39.6 ± 6.7*	46.5 ± 9.6	38.9 ± 5.7	48.0 ± 5.1	40.1 ± 7.1##	0.99
	Trait anxiety (STAI-II)	45.0 ± 8.00	42.2 ± 9.3	48.5 ± 9.2	47.2 ± 10.4	47.2 ± 8.9	46.5 ± 10.6	0.93
	Depression (SRQ-D)	10.1 ± 4.00	10.5 ± 5.2	11.1 ± 3.9	9.0 ± 5.3	8.7 ± 3.0	8.2 ± 3.0	0.62
SOHSI	Ability to chew (AC)	15.3 ± 19.7	6.4 ± 8.4	10.6 ± 15.4	3.0 ± 6.7	14.2 ± 14.9	9.5 ± 18.8	0.91
	Ability to speak (AS)	58.9 ± 38.8	17.9 ± 32.2	51.5 ± 45.6	18.1 ± 22.9	38.0 ± 44.8	38.0 ± 48.7	0.27
	Oral and facial pain symptoms (OFPS)	16.4 ± 20.9	13.1 ± 13.6	18.1 ± 14.4	22.0 ± 16.1	12.2 ± 20.9	22.4 ± 13.9	0.47
	Other oral symptoms (OOS)	15.3 ± 14.5	16.1 ± 12.6	20.0 ± 8.9	16.3 ± 12.0	18.5 ± 10.6	14.2 ± 12.7	0.76
	Eating impact scale (EIS) (%)	67.7 ± 37.0	38.7 ± 35.5*	66.6 ± 42.1	36.3 ± 37.8	61.9 ± 40.4	38.0 ± 35.6	0.96
	Eating impact scale (EIS) (sum)	11.0 ± 3.0	13.4 ± 1.5**	11.5 ± 2.9	13.6 ± 1.4+	12.1 ± 1.7	12.1 ± 2.8	0.32
	Communication/social relations impact scale (CSIS) (%)	48.0 ± 27.8	25.0 ± 22.8**	52.2 ± 3.9	13.6 ± 20.5++	46.4 ± 22.4	32.1 ± 34.5	0.43
	Communication/social relations impact scale (CSIS) (sum)	16.9 ± 2.30	18.6 ± 1.8	15.9 ± 3.6	19.3 ± 1.0+	16.4 ± 2.2	18.4 ± 1.9#	0.41
	Activities daily living impact scale (ADIS) (%)	30.7 ± 33.9	19.2 ± 34.5	27.2 ± 36.7	4.5 ± 10.7	26.1 ± 26.9	11.9 ± 18.5	0.80
	Activities daily living impact scale (ADIS) (sum)	27.2 ± 3.10	28.7 ± 2.2*	27.8 ± 3.1	29.7 ± 0.6	28.1 ± 2.3	29.1 ± 1.4	0.87
	Worry/concern impact scale (WCIS) (%)	96.1 ± 13.8	50.0 ± 28.8*	81.8 ± 25.2	63.6 ± 45.2	92.8 ± 18.8	71.4 ± 26.7	0.20
	Worry/concern impact scale (WCIS) (sum)	6.00 ± 1.70	9.0 ± 0.5**	5.60 ± 2.9	8.0 ± 1.9+	5.8 ± 2.1	7.4 ± 2.2	0.60
OQLQ	Social aspects of dentofacial deformity (SA)	10.0 ± 6.6	3.4 ± 4.3*	12.4 ± 10.0	4.7 ± 5.4+	13.1 ± 11.1	6.2 ± 5.7	0.96
	Facial aesthetics (FA)	9.10 ± 5.0	2.5 ± 2.9*	11.2 ± 5.1	3.1 ± 3.4++	9.2 ± 5.5	3.8 ± 3.9	0.66
	Oral function (OF)	11.8 ± 5.4	5.9 ± 4.3*	13.7 ± 6.5	8.8 ± 5.1+	14.7 ± 6.7	7.8 ± 5.7#	0.87
	Awareness of dentofacial aesthetics (ADFA)	7.20 ± 3.6	4.6 ± 3.9	7.50 ± 5.5	6.0 ± 5.4	6.2 ± 4.6	5.0 ± 3.4	0.89
RSS-M	Recognition	22.1 ± 4.6	10.8 ± 4.5**	25.6 ± 7.1	14.7 ± 7.7++	24.7 ± 4.9	15.4 ± 7.7#	0.88
	Satisfacion	18.7 ± 4.2	30.6 ± 7.5**	15.5 ± 6.0	30.3 ± 6.4++	17.7 ± 5.9	30.4 ± 5.5#	0.71

Generic quality of life was measured by SF-36 (The MOS Short Form-36). Psychological status was measured by STAI (State-Trait Anxiety Inventory Questionnaire) and SRQ-D (Self-Rating Questionnaire for Depression). Disease specific quality of life was measured by SOHSI (The Subjective Oral Health Indicators), OQLQ (The Orthognathic Quality of Life Questionnaire), and RSS-M (The Recognition and Satisfaction scale Modified). T1: before surgery, T2: after debonding of multibracket appliance. SS: Severity score. Low-SS: SS 2-4, Moderate-SS: SS 5, High-SS: SS 6-7. Results expressed as mean ± standard error (median). *Significantly different from T1 two-way factorial ANOVA; $p < 0.05$. **Significantly different from T1 by two-way factorial ANOVA; $p < 0.01$. +Significantly different from Moderate-SS (T1) by two-way factorial ANOVA; $p < 0.05$. ++Significantly different from Moderate-SS (T1) by two-way factorial ANOVA; $p < 0.01$. #Significantly different from High-SS (T1) by two-way factorial ANOVA; $p < 0.05$. ##Significantly different from High-SS (T1) by two-way factorial ANOVA; $p < 0.01$.

TABLE 5. Variables related to QOL scales in a stepwise logistic regression.

	C-R^2 (%)	p	Variables entered in equation	F
STAI-I (T2)	1.0	0.2652	ADFA (T1)	1.291
STAI-II (T2)	53.6	< 0.0001	STAI-II (T1)	34.649
			STAI-I (T1)	7.236
SRQ-D (T2)	31.6	0.0019	SRQ-D (T1)	14.388
			STAI-I (T1)	4.75
SA (T2)	28.5	0.0012	SA (T1)	12.963
FA (T2)	32.1	0.0064	OF (T1)	11.007
			SA (T1)	6.012
			STAI-I (T1)	4.801
			STAI-II (T1)	4.448
OF (T2)	35.0	0.0021	STAI-I (T1)	9.108
			STAI-II (T1)	8.538
			Gender	6.812
ADFA (T2)	34.5	0.001	ADFA (T1)	10.609
			STAI-I (T1)	6.441
Recognition (T2)	10.1	0.0456	Recognition (T1)	4.365
Satisfaction (T2)	25.1	0.0066	Age	8.681
			Recognition (T1)	4.647

Logistic regression analysis was performed with the psychological status and the disease-specific QOL after surgery. Psychological status was measured by STAI (State-Trait Anxiety Inventory Questionnaire) and SRQ-D (Self-Rating Questionnaire for Depression). Disease specific quality of life was measured by OQLQ (The Orthognathic Quality of Life Questionnaire), and RSS-M (The Recognition and Satisfaction scale Modified). T1: before surgery, T2: after debonding of multibracket appliance. STAI-I; state anxiety, STAI-II; trait anxiety, SRQ-D; depression, SA; social aspects of dentofacial deformity, FA; facial aesthetics, OF; oral function, ADFA; awareness of dentofacial aesthetics.

regression was applied (Table 5), the predictor of postoperative "Recognition" was the preoperative "Recognition" (10.1%, $p < 0.05$), and the predictor of postoperative "Satisfaction" was the preoperative age and "Recognition" (25.1%, $p < 0.01$).

Comparisons of HRQOL and psychological status in High-anxiety and Low-anxiety

The HRQOL and psychological status of patients divided into two groups according to the anxiety level is shown Fig. 2. There was no interaction between the groups in any of the domains. "STAI-I" improved significantly after the treatment in both groups. However, "STAI-II" did not change significantly.

Comparisons of HRQOL and psychological status in High-depression and Low-depression level

The HRQOL and psychological status of patients divided into two groups according to the depression level is shown in Fig. 3. There was no interaction. "SRQ-D" did not improve significantly after the treatment in the two groups.

DISCUSSION

In the present study, the improvement of disease-specific HRQOL and psychological status of patients with malocclusion after the surgical correction was demonstrated irrespective of the severity before surgery. In contrast, no change was recognized in generic HRQOL after the treat-

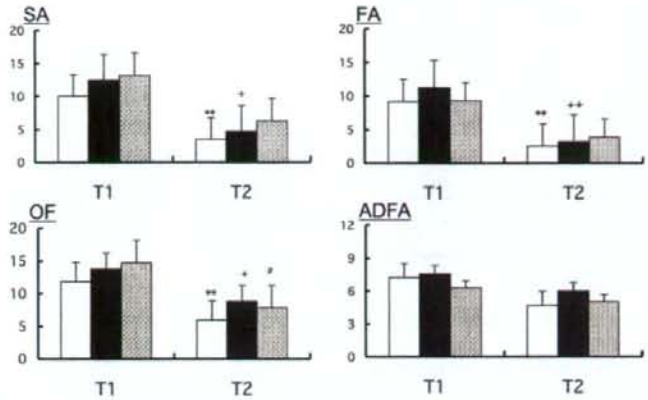

Fig. 1. Comparisons of disease specific quality of life measured by OQLQ among Low-SS, Moderate-SS and High-SS.
Results expressed as mean ± standard error (S.E.M.). □, Low-SS; ■, Moderate-SS, ▨, High-SS. Disease specific quality of life was measured by OQLQ (The Orthognathic Quality of Life Questionnaire). T1: before surgery, T2: after debonding of multibracket appliance. Results expressed as mean ± standard error (S.E.M.). SA, social aspects of dentofacial deformity; FA, facial aesthetics; OF, oral function; ADFA, awareness of dentofacial aesthetics.
**Significantly different from Low-SS (T1) by two-way factorial ANOVA; $p < 0.01$.
+Significantly different from Moderate-SS (T1) by two-way factorial ANOVA; $p < 0.05$.
++Significantly different from Moderate-SS (T1) by two-way factorial ANOVA; $p < 0.01$.
#Significantly different from High-SS (T1) by two-way factorial ANOVA; $p < 0.05$.

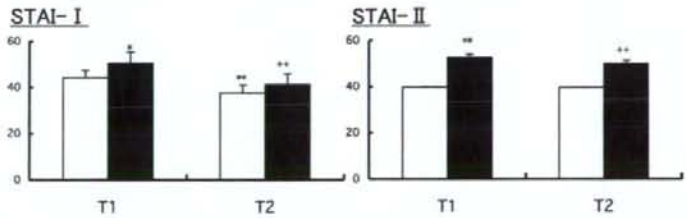

Fig. 2. Comparisons of anxiety level measured by STAI among Low-anxiety and High-anxiety.
Results expressed as mean ± standard error (S.E.M.). □, Low-anxiety; $n = 15$, anxiety score 30-46, ■, High-anxiety; $n = 16$, anxiety score 47-67. Psychological status was measured by STAI (State-Trait Anxiety Inventory Questionnaire). T1: before surgery, T2: after debonding of multibracket appliance. Results expressed as mean ± standard error (S.E.M.). STAI- I; state anxiety, STAI- II; trait anxiety.
*Significantly different from Low-anxiety (T1) by two-way factorial ANOVA; $p < 0.05$.
**Significantly different from Low-anxiety (T1) by two-way factorial ANOVA; $p < 0.01$.
++Significantly different from High-anxiety (T1) by two-way factorial ANOVA; $p < 0.01$.

ment. The patients' state anxiety improved after the treatment irrespective of their individual anxiety and depression level before surgery. In contrast, trait anxiety and depression were unchanged. Moreover, both postoperative anxiety and HRQOL were determined to a certain extent by the preoperative anxiety and HRQOL.

This is the first report addressing the